PROCEEDINGS OF SCIENCE

Modeling of the galactic cosmic-ray anisotropy at TeV energies using an intensity-mapping method in an MHD model heliosphere

T. K. Sako,* on behalf of the Tibet ASγ collaboration, and N. V. Pogorelov[†]

It has been established by high-statistics cosmic-ray experiments that the distribution of arrival directions of TeV cosmic rays have small anisotropic features with amplitudes of ∼0.1%. In this presentation, we use the intensity-mapping method based on Liouville's theorem for the modeling of the TeV cosmic-ray anisotropy. Our results derived from the data of the Tibet ASγ experiment and the calculation of cosmic-ray trajectories in an MHD model heliosphere indicate that the relative intensity distibution of cosmic rays at the outer boundary of the heliosphere contains small-scale ansiotropic features with angular scales of smaller than ∼10°, which does not seem realistic. A possible problem would be that the MHD model heliosphere used in this presentation is a single snapshot of the positive polarity phase of a solar cycle, while the experimental data covers ten years during the negative polarity phase of the 23rd solar cycle. In order to improve our intensity-mapping method, it would be necessary to have multiple snapshots of the MHD model heliosphere corresponding to the negative polarity phase, perform the intensity-mapping for each of the snapshots and take the average of the results.

38th International Cosmic Ray Conference (ICRC2023)
26 July - 3 August, 2023
Nagoya, Japan

[†]Department of Space Science and Center for Space Plasma and Aeronomic Research, University of Alabama in Huntsville, 320 Sparkman Drive, Huntsville, AL 35899, USA
*Speaker

PoS(ICRC2023)1238

1. Introduction

Arrival directions of galactic cosmic rays observed at the Earth are not completely uniform. At TeV energies some recent high-statistics experiments (e.g. [1–6]) have reported small yet significant anisotropic features with amplitudes of roughly 0.1%, such as a large-scale deficit region called 'Loss-Cone' and an excess region called 'Tail-In'. The origins of these structures have not been known yet, although the anisotropy is considered to reflect how cosmic rays propagate through magnetic fields in the heliosphere and the surrounding interstellar medium.

Some recent studies [7, 8] make use of the 'intensity-mapping' method, in which heliospheric magnetic field structures are reconstructed by MHD simulations, trajectories of cosmic rays are calculated in the MHD model heliosphere, and the cosmic-ray intensity distribution observed at the Earth is mapped back onto that at the outer boundary based on Liouville's theorem. Then, the intensity distribution at the outer boundary is modeled by a superposition of particle flows and interpreted in physical terms. Using the cosmic-ray anisotropy observed by the Tibet ASγ experiment [1], the latest work [8] indicated that, in the interstellar medium outside the heliosphere, the flow of cosmic rays along the interstellar magnetic field ($B_{\rm ISM}$) is dominant, and that there is a density gradient of cosmic rays in the direction of Vela, the nearest known supernova remnant at a distance of 815 light years from the Earth. To establish a conclusive modeling, however, there are at least two technical issues to overcome. Firstly, the previous work [8] discussed cosmic-ray flows in the interstellar medium based on their intensity-mapping method in which 4 TeV mono-energy protons were shot from the Earth, although the acceleration and deceleration of those protons in the MHD model heliosphere were taken into account. Cosmic rays observed at the Earth by the Tibet ASγ experiment, however, are composed of a variety of atomic nuclei with different energies. One needs to take into account the energy spectrum and the composition of observed cosmic rays in the intensity-mapping process. Secondly, the χ^2/ndf (number of degrees of freedom) value of the fitting between the experimental and model anisotropies was 4.5 in the previous work, which was not sufficiently good. One needs to improve the model of the intensity distribution at the outer boundary so that the χ^2/ndf value becomes approximately unity.

2. Intensity Mapping Method

The data used in this presentation was taken by the Tibet ASγ experiment from November 1999 to May 2010, which corresponds to the negative polarity phase of the 23rd solar cycle. For the pixelization of the sky we use the HEALPix algorithm [9] with $N_{\rm side} = 16$, which divides the sky in our field of view ($-20^\circ <$ decl. $< 80^\circ$) in 2056 pixels, each of which has an approximate size of $3.7^\circ \times 3.7^\circ$.

We have performed detailed MC simulations of air-shower generation and detector response to estimate the rigidity distribution of cosmic rays observed by the experiment. Using a model of the energy spectrum and the cosmic-ray chemical composition based on direct measurements [10], we generate air showers in the energy range from 0.3 TeV and 10 PeV using CORSIKA v7.4000 [11] with EPOS LHC [12] for the high-energy hadronic interaction model and FLUKA v2011.2b [13, 14] for the low-energy hadronic interaction model. The generated air showers are fed into the detector response simulation developed by GEANT v4.10.00 [15] and analyzed in the same way as

in the experiment. Figure 1 shows the obtained rigidity distribution of cosmic rays detected by the experiment for five typical declination bands.

Cosmic-ray trajectories in the MHD model heliosphere are calculated with the fourth-order Runge-Kutta method. The Earth is set at four positions around the Sun at a distance of 1 AU on the ecliptic plane to smooth out possible seasonal effects. The sky in the declination range from -20° to 80° is pixelized with $N_{\rm side} = 32$, and from the center of each pixel cosmic-ray particles are shot into the MHD model heliosphere with their charges reversed and with their rigidity spectra as shown in Figure 1. The MHD model heliosphere that we use for cosmic-ray trajectory calculation in this presentation is identical to the one employed in the previous work [8]. After tracking the particles in the MHD model heliosphere, their momentum directions are recorded at the boundaries defined in Figure 2. Then we set the intensity for a particle momentum direction at the outer boundary ($I_{\rm ISM}$) to be equal to that at the Earth ($I_{\rm E}$). The outermost boundary is indicated by a solid black line, which is a surface where the deviation of the magnetic field strength (direction) from that outside the heliosphere becomes smaller than 0.1% (0.1°). In this presentation, the cosmic-ray relative intensity distribution is evaluated at three boundaries at distances of 630 AU, 1580 AU and 3980 AU from the Sun as indicated by dotted lines in Figure 2.

The experimental data has the declination bias — the average intensity in each declination band is normalized to unity, because the detection efficiency of the experiment along the declination direction has not been calibrated absolutely. For this reason, deriving the $I_{\rm ISM}$ distribution at the outer boundary is not straightforward. We take the following steps: 1) set up a model of the distribution of the cosmic-ray intensity at the outer boundary $I_{\rm ISM}$, 2) map $I_{\rm ISM}$ to that at the Earth $I_{\rm E}$, 3) normalize the average of $I_{\rm E}$ in each declination band to unity, and 4) calculate χ^2 between the normalized $I_{\rm E}$ and the experimental data. Repeating 1) to 4), we obtain the best-fit model of $I_{\rm ISM}$ that minimizes χ^2. At step 1), we assume the relative intensity distribution at the outer boundary in a series of spherical harmonics Y_{lm} as:

$$I_{\rm ISM} = 1 + \sum_{l=1}^{l_{\rm max}} \sum_{m=-l}^{l} f_{lm} Y_{lm} + I_{\rm CG}, \tag{1}$$

where f_{lm}'s are free fitting parameters.

3. Results and Discussions

Figure 3 shows the summary of the results. Panel (a) shows the experimental data. Panels (b), (d) and (f) are the best-fit model relative intensity distributions at the Earth when we take the outer boundaries at distances of 630 AU, 1580 AU and 3980 AU from the Sun, respectively. Panels (c), (e) and (g) are the best-fit model relative intensity distributions at the outer boundaries at distances of 630 AU, 1580 AU and 3980 AU from the Sun, respectively. The maximum order $l_{\rm max}$ of the spherical harmonics Y_{lm} in Eq.(1) is increased until the fitting χ^2/ becomes reasonably small; $l_{\rm max} = 4$ for Panels (b)(c), $l_{\rm max} = 8$ for Panels (d)(e), and $l_{\rm max} = 20$ for Panels (f)(g), and the obtained χ^2/ndf values are 0.96 (89%), 0.98 (71%) and 0.94 (95%), respectively. Panels (c), (e) and (g) in Figure 3 show that $l_{\rm max}$ increases as the boundary goes farther from the Sun. We naturally assume in terms of physics that the cosmic-ray intensity distribution outside the heliosphere has only large-scale

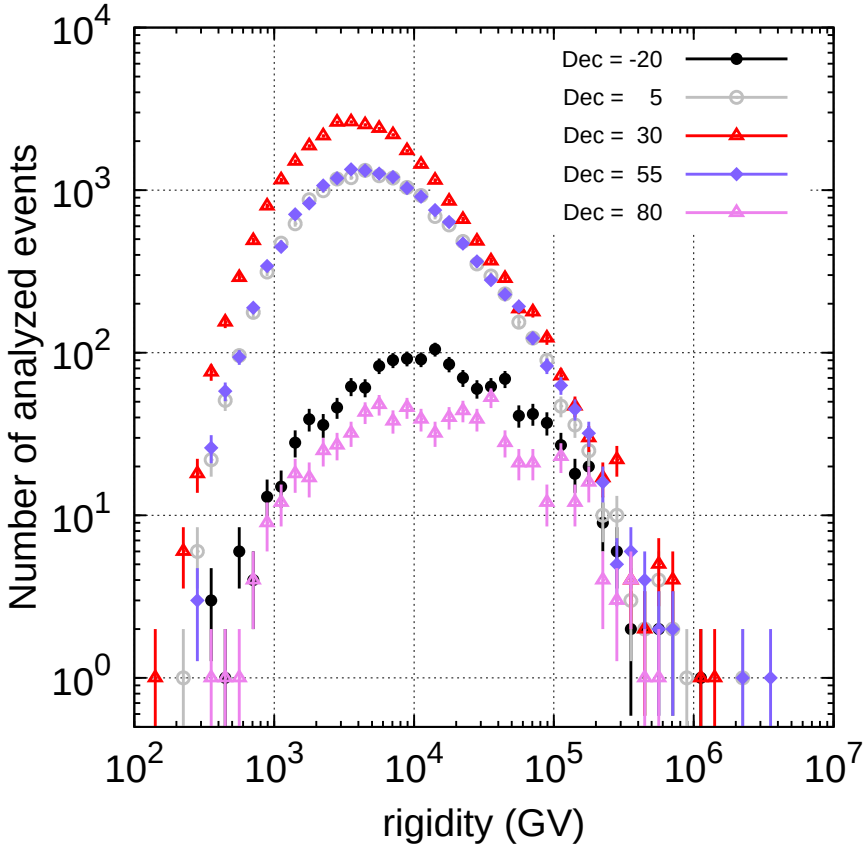

Figure 1: Rigidity distribution of cosmic rays observed by the Tibet ASγ experiment for five typical declination bands, reproduced from MC simulations.

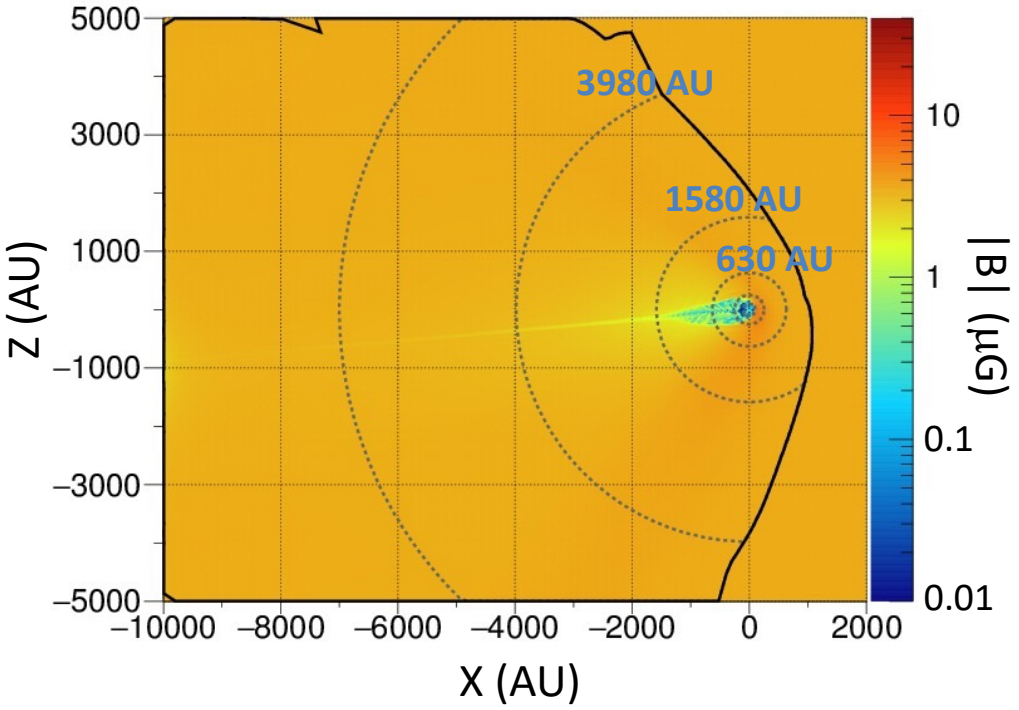

Figure 2: Distribution of the magnetic field strength of the MHD model heliosphere employed in this work. The black solid line and the dotted circles indicate the outer boundaries of the intensity mapping.

anisotropic features, and that the heliospheric modulation of cosmic-ray trajectories adds small-scale anisotropic features to the intensity distribution. The tendency indicated by panels (c), (e) and (g), however, is quite contrary to this natural assumption. Therefore, our intensity-mapping method would need more improvement. A possible problem would be that the MHD model heliosphere used in this presentation is a single snapshot of the positive polarity phase of a solar cycle, while the experimental data covers ten years during the negative polarity phase of the 23rd solar cycle. It would be necessary to have multiple snapshots of the MHD model heliosphere corresponding to the negative polarity phase, perform the intensity-mapping for each of the snapshots and take the average of the results.

References

[1] M. Amenomori *et al.*, Science, **314**, 439 (2006)
[2] M. Amenomori *et al.*, Astrophys. Space Sci. Trans., **6**, 49 (2010)
[3] B. Bartoli *et al.*, Astrophys. J., **809**, 90 (2015)
[4] M. G. Aartsen *et al.*, Astrophys. J., **826**, 220 (2016)
[5] A. U. Abeysekara *et al.*, Astrophys. J., **865**, 57 (2018)

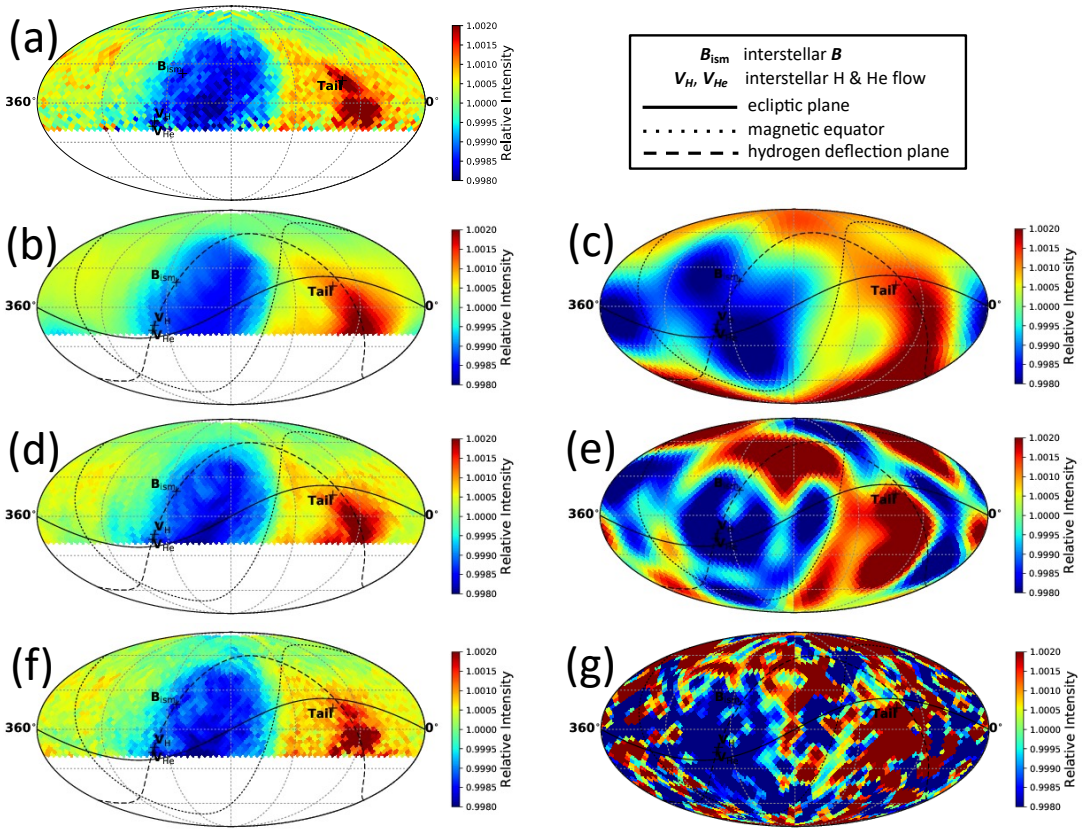

Figure 3: Panel (a) shows the experimental data. Panels (b), (d), (f) are the best-fit model relative intensity distributions at the Earth when we take the outer boundaries at distances of 630 AU, 1580 AU and 3980 AU from the Sun, respectively. Panels (c), (e), (g) are the best-fit model relative intensity distributions at the outer boundaries at distances of 630 AU, 1580 AU and 3980 AU from the Sun, respectively.

[6] A. U. Abeysekara *et al.*, Astrophys. J., **871**, 96 (2019)
[7] M. Zhang *et al.*, Astrophys. J., **790**, 5 (2014)
[8] M. Zhang *et al.*, Astrophys. J., **889**, 97 (2020)
[9] K. M. Górski *et al.*, Astrophys. J., **622**, 759 (2005)
[10] M. Shibata *et al.*, Astrophys. J., **716**, 1076 (2010)
[11] D. Heck *et al.*, CORSIKA: a Monte Carlo Code to Simulate Extensive Air Showers Report FZKA-6019 (Forschungszentrum Karlsruhe, 1998)
[12] T. Pierog *et al.*, Phys. Rev. C, **92**, 034906 (2015)
[13] T. T. Böhlen *et al.*, Nucl. Data Sheets, **120**, 211 (2014)
[14] A. Ferrari *et al.*, Report CERN-2005-10, INFN/TC_05/11, SLAC-R-773 (CERN European Organization for Nuclear Research, 2005)
[15] S. Agostinelli *et al.*, Nucl. Instrum. Meth. A, **506**, 250 (2003)
[16] K. Munakata *et al.*, Astrophys. J., **712**, 1100 (2010)

Acknowledgements

The collaborative experiment of the Tibet Air Shower Arrays has been conducted under the auspices of the Ministry of Science and Technology of China and the Ministry of Foreign Affairs of Japan. This work was supported in part by a Grant-in-Aid for Scientific Research on Priority Areas from the Ministry of Education, Culture, Sports, Science and Technology, and by Grants-in-Aid for Science Research from the Japan Society for the Promotion of Science in Japan. This work is supported by the National Natural Science Foundation of China under Grants No. 12227804, No. 12275282, No. 12103056 and No. 12073050, and the Key Laboratory of Particle Astrophysics, Institute of High Energy Physics, CAS. This work is also supported by the joint research program of the Institute for Cosmic Ray Research (ICRR), the University of Tokyo.

Full Authors List: the Tibet ASγ Collaboration

M. Amenomori[1], Y. W. Bao[2], X. J. Bi[3], D. Chen[4], T. L. Chen[5], W. Y. Chen[3], Xu Chen[4], Y. Chen[2], Cirennima[5], S. W. Cui[6], Danzengluobu[5], L. K. Ding[3], J. H. Fang[3,7], K. Fang[3], C. F. Feng[8], Zhaoyang Feng[3], Z. Y. Feng[9], Qi Gao[5], Q. B. Gou[3], Y. Q. Guo[3], Y. Y. Guo[3], Y. Hayashi[10], H. H. He[3], Z. T. He[6], K. Hibino[11], N. Hotta[12], Haibing Hu[5], H. B. Hu[3], K. Y. Hu[3,7], J. Huang[3], H. Y. Jia[9], L. Jiang[3], P. Jiang[4], H. B. Jin[4], K. Kasahara[13], Y. Katayose[14], C. Kato[10], S. Kato[15], I. Kawahara[14], T. Kawashima[15], K. Kawata[15], M. Kozai[16], Labaciren[5], G. M. Le[17], A. F. Li[3,9,18], H. J. Li[5], W. J. Li[3,10], Y. Li[4], Y. H. Lin[3,7], B. Liu[19], C. Liu[3], J. S. Liu[3], L. Y. Liu[4], M. Y. Liu[5], W. Liu[3], H. Lu[3], T. Makishima[14], Y. Masuda[10], S. Matsuhashi[14], M. Matsumoto[10], X. R. Meng[5], Y. Meng[3,7], A. Mizuno[15], K. Munakata[10], Y. Nakamura[15], H. Nanjo[1], C. C. Ning[5], M. Nishizawa[20], R. Noguchi[14], M. Ohnishi[15], S. Okukawa[14], S. Ozawa[21], X. Qian[4], X. L. Qian[22], X. B. Qu[23], T. Saito[24], M. Sakata[25], T. Sako[15], T. K. Sako[15], T. Sasaki[11], J. Shao[3,9], T. Shibasaki[26], M. Shibata[14], A. Shiomi[26], H. Sugimoto[27], W. Takano[11], M. Takita[15], Y. H. Tan[3], N. Tateyama[11], S. Torii[28], H. Tsuchiya[29], S. Udo[11], R. Usui[14], H. Wang[3], S. F. Wang[5], Y. P. Wang[5], Wangdui[5], H. R. Wu[3], Q. Wu[5], J. L. Xu[4], L. Xue[8], Z. Yang[3], Y. Q. Yao[4], J. Yin[4], Y. Yokoe[15], Y. L. Yu[3,7], A. F. Yuan[5], L. M. Zhai[4], H. M. Zhang[3], J. L. Zhang[3], X. Zhang[2], X. Y. Zhang[8], Y. Zhang[3], Yi Zhang[30], Ying Zhang[3], S. P. Zhao[3], Zhaxisangzhu[5], X. X. Zhou[9] and Y. H. Zou[3,7]

[1]Department of Physics, Hirosaki University, Hirosaki 036-8561, Japan.
[2]School of Astronomy and Space Science, Nanjing University, Nanjing 210093, China.
[3]Key Laboratory of Particle Astrophysics, Institute of High Energy Physics, Chinese Academy of Sciences, Beijing 100049, China.
[4]National Astronomical Observatories, Chinese Academy of Sciences, Beijing 100101, China.
[5]Department of Mathematics and Physics, Tibet University, Lhasa 850000, China.
[6]Department of Physics, Hebei Normal University, Shijiazhuang 050016, China.
[7]University of Chinese Academy of Sciences, Beijing 100049, China.
[8]Institute of Frontier and Interdisciplinary Science and Key Laboratory of Particle Physics and Particle Irradiation (MOE), Shandong University, Qingdao 266237, China.
[9]Institute of Modern Physics, SouthWest Jiaotong University, Chengdu 610031, China.
[10]Department of Physics, Shinshu University, Matsumoto 390-8621, Japan.
[11]Faculty of Engineering, Kanagawa University, Yokohama 221-8686, Japan.
[12]Faculty of Education, Utsunomiya University, Utsunomiya 321-8505, Japan.
[13]Faculty of Systems Engineering, Shibaura Institute of Technology, Omiya 330-8570, Japan.
[14]Faculty of Engineering, Yokohama National University, Yokohama 240-8501, Japan.
[15]Institute for Cosmic Ray Research, University of Tokyo, Kashiwa 277-8582, Japan.
[16]Polar Environment Data Science Center, Joint Support-Center for Data Science Research, Research Organization of Information and Systems, Tachikawa 190-0014, Japan.
[17]National Center for Space Weather, China Meteorological Administration, Beijing 100081, China.
[18]School of Information Science and Engineering, Shandong Agriculture University, Taian 271018, China.
[19]Department of Astronomy, School of Physical Sciences, University of Science and Technology of China, Hefei 230026, China.
[20]National Institute of Informatics, Tokyo 101-8430, Japan.
[21]National Institute of Information and Communications Technology, Tokyo 184-8795, Japan.
[22]Department of Mechanical and Electrical Engineering, Shangdong Management University, Jinan 250357, China.
[23]College of Science, China University of Petroleum, Qingdao 266555, China.
[24]Tokyo Metropolitan College of Industrial Technology, Tokyo 116-8523, Japan.
[25]Department of Physics, Konan University, Kobe 658-8501, Japan.
[26]College of Industrial Technology, Nihon University, Narashino 275-8575, Japan.
[27]Shonan Institute of Technology, Fujisawa 251-8511, Japan.
[28]Research Institute for Science and Engineering, Waseda University, Tokyo 162-0044, Japan.
[29]Japan Atomic Energy Agency, Tokai-mura 319-1195, Japan.
[30]Key Laboratory of Dark Matter and Space Astronomy, Purple Mountain Observatory, Chinese Academy of Sciences, Nanjing 210034, China.

PoS(ICRC2023)1238